Eur Respir J 2010; 36: 170–177
DOI: 10.1183/09031936.00136709

Human airway smooth muscle is structurally and mechanically similar to that of other species

L.Y.M. Chin*,#, Y. Bossé#, Y. Jiao#, D. Solomon#, T.L. Hackett#,¶, P.D. Paré#,+ and C.Y. Seow*,#

ABSTRACT: Airway smooth muscle (ASM) plays a vital role in the exaggerated airway narrowing seen in asthma. However, whether asthmatic ASM is mechanically different from nonasthmatic ASM is unclear. Much of our current understanding about ASM mechanics comes from measurements made in other species. Limited data on human ASM mechanics prevents proper comparisons between healthy and asthmatic tissues, as well as human and animal tissues. In the current study, we sought to define the mechanical properties of healthy human ASM using tissue from intact lungs and compare these properties to measurements in other species.

The mechanical properties measured included: maximal stress generation, force–length properties, the ability of the muscle to undergo length adaptation, the ability of the muscle to recover from an oscillatory strain, shortening velocity and maximal shortening. The ultrastructure of the cells was also examined.

Healthy human ASM was found to be mechanically and ultrastructurally similar to that of other species. It is capable of undergoing length adaptation and responds to mechanical perturbation like ASM from other species. Force generation, shortening capacity and velocity were all similar to other mammalian ASM.

These results suggest that human ASM shares similar contractile mechanisms with other animal species and provides an important dataset for comparisons with animal models of disease and asthmatic ASM.

KEYWORDS: Airway hyperresponsiveness, asthma, force–length relationship, force–velocity relationship, shortening, ultrastructure

AFFILIATIONS
Depts of *Pathology and Laboratory Medicine,
¶Anesthesiology, Pharmacology and Therapeutics, and
+Experimental Medicine, St. Paul's Hospital, University of British Columbia, and
#The James Hogg iCAPTURE Centre for Cardiovascular and Pulmonary Research, St. Paul's Hospital, University of British Columbia, Vancouver, BC, Canada.

CORRESPONDENCE
L.Y.M. Chin
iCAPTURE Centre
St. Paul's Hospital
166–1081 Burrard Street
Vancouver
BC
V6Z 1Y6
Canada
E-mail: lchin@mrl.ubc.ca

Received:
Aug 28 2009
Accepted after revision:
Nov 01 2009
First published online:
Nov 19 2009

While the physiological function of airway smooth muscle (ASM) is unclear [1–3], its contraction and subsequent shortening act to increase airway resistance in the lung. Asthma is characterised by episodes of increased airway resistance due to exaggerated airway narrowing. Although it is generally agreed that the narrowing is caused by ASM shortening, it is still unclear if the excessive narrowing is due to fundamental changes in the phenotype of the smooth muscle itself, or if it is caused by structural and/or mechanical changes in the noncontractile elements of the airway wall, or by alterations in the relationship of the airway wall to the surrounding lung parenchyma [4]. One major hurdle in determining whether ASM is truly dysfunctional in asthma is the lack of adequate data on the mechanical properties of human ASM. Much of our current knowledge about ASM contractile function has come from studies in other mammalian species, which may not adequately represent human tissue. Hence, in order to investigate a potential role for ASM in asthma, it is first necessary to characterise the mechanical properties of nonasthmatic ASM. Since many hypotheses concerning the pathogenesis of asthma have been developed from animal models, it is necessary to determine the relevance of these animal models with respect to human tissues. Thus, the goal of this study was to describe the mechanical properties and ultrastructure of nonasthmatic ASM and compare the data to previous human and mammalian studies of this tissue.

In the relatively few descriptions of nonasthmatic human ASM properties, a consistent finding has been higher passive tension, lower active force (and stress) and less shortening, compared with ASM preparations from other animal species [5, 6]. However, the results of these studies may be limited, owing to the fact that the tissues were

European Respiratory Journal
Print ISSN 0903-1936
Online ISSN 1399-3003

TABLE 1 Subject demographics and clinical details

Sex	Age yrs	Weight kg	Height cm	Ethnicity	Cause of death	Medical history	Known medications	Terminal medications
Male	4	17.5	104	Hispanic	Head trauma	None	None	Steroids and vasopressors
Male	22	112	193	Caucasian	Head trauma	Occasional marijuana use (once a year)	None	Vasopressors
Female	63	77	159	Caucasian	Gastrointestinal bleed	Hypertension for 2 yrs	Unknown antihypertensive	Dopamine
Female	19	87	165	Caucasian	Head trauma	None	None	Steroids and vasopressors
Female	20	72.2	165	Caucasian	Head trauma	Smoked cigarettes <1 PPD for 2 yrs; smoked marijuana (unknown frequency)	Pain medications and inhalants	Vasopressors
Male	24	81.8	175	Hispanic	Head trauma	None	None	Vasopressors

PPD: pack per day.

obtained mostly from bronchial surgical resections [5–22]. In the current study, the ASM was carefully dissected from the tracheas of intact lungs donated for research.

Besides measuring the ''classical'' force–length and force–velocity relationships, we have focused on a newly recognised property of ASM, namely its plastic adaptability to the dynamic lung environment. None of the previous studies on mechanical properties of human ASM have studied plastic adaptation of the tissue. Importantly, in this study we used the *in situ* muscle length as the reference length for the muscle instead of the previous convention of L_{max} (the length at which force was maximal at a given instant) [23].

MATERIALS AND METHODS

Tissue preparation and equilibration

Tracheas were removed from nontransplantable human lungs donated for research through the International Institute for the Advancement of Medicine (Edison, NJ, USA). All donors had no known respiratory disease and their deaths were sudden. The subject demographics and clinical details are shown in table 1. The study was approved by the University of British Columbia/St Paul's Hospital ethics committee. The whole lungs were obtained as previously described [24]. Briefly, after surgical removal the lungs were flushed with Custodiol HTK solution (Odyssey Pharmaceuticals, East Hanover, NJ, USA) and transported by plane on ice. The average time between harvesting and arrival at the University of British Columbia was 15–20 h.

The procedure of dissection and preparation of the smooth muscle was the standard procedure for sheep tissue and has been previously described, for details see [25, 26]. Briefly, the tracheal tissue was kept at 4°C in physiological saline solution (PSS). Dissection was undertaken within a day of obtaining the tissue. The *in situ* length of the tracheal smooth muscle was used as a reference length (L_{ref}), which was determined prior to cutting open the C-shaped cartilage ring. Connective tissue and epithelium was carefully removed to isolate a smooth muscle bundle. Muscle strips measuring 1–1.5 mm wide, 0.5 mm thick and 6 mm long, were attached on both ends with aluminum foil clips and mounted vertically on a force–length transducer. Before beginning the experimental protocol, the muscle was equilibrated at L_{ref} by periodic electrical field stimulation (EFS) at 5-min intervals for a period of 1.5 h. Since some tissues exhibited substantial leukotriene-mediated tone without extrinsic stimulation, the CysLT1 receptor antagonist montelukast (10^{-6} M) was added to the PSS for all of the experiments, which prevented or eliminated tone.

Mechanical measurements

After equilibration, the maximal isometric force produced in response to EFS at L_{ref} was determined (herein called F_{max}). For the force–length relationship the muscle was either stretched or shortened in a stepwise fashion as previously described [25, 27] and allowed to adapt to every new length for 20 min, during which it was stimulated with EFS at 5-min intervals. Five different lengths were examined: 0.5, 0.75, 1.0, 1.25, and 1.5 L_{ref}. To determine the response to length perturbation, a 10 min, 0.2 Hz, 30% L_{ref} length oscillation was applied. The recovery of EFS-induced (active) force was followed for 30 min after oscillation by stimulating with EFS at 5-min intervals. For the force–velocity curves, velocity measurements were made after release (quick switch from isometric to isotonic contraction) at five graded loads (between zero and F_{max}) at L_{ref}, as previously described [28]. Velocities were measured at two time points: one at the peak of tetanic force and one mid-way to the peak. This is due to the nonlinear nature of shortening velocity, which peaks early on as developed force reaches ~50% of F_{max}, and settles to a lower plateau after the force reaches F_{max} [29]. Shortening velocity against a given load was recorded 100 ms after the release, during the steady phase of shortening. The curves were fit using Hill's hyperbolic equation [30]. Maximal isotonic shortening was established by allowing a muscle to contract against a preload equal to 10% and 20% F_{max}. It was not possible to perform the shortening at zero load, because the servo-system of the myograph became unstable at low loads. Therefore, the maximal shortening was extrapolated to zero load from these two points.

Histology and electron microscopy

At the end of the mechanical protocols the tissue preparations were fixed at L_{ref} in 10% formalin for histology or a formaldehyde cocktail for transmission electron microscopy (EM).

The histology was performed as previously described [31]. The amount of muscle in the preparation was determined by staining transverse sections with Masson's trichrome and quantified by manual tracing using Image ProPlus 4.5 (MediaCybernetics, Bethesda, MD, USA). Maximal stress generating capacity was determined by dividing F_{max} (in mN) by the cross-sectional area (in mm^2) of muscle present in the preparation. The protocol for EM followed the standard procedure previously described in our lab [32].

Statistical analysis

Force and length measurements were normalised to F_{max} or L_{ref}, respectively, and expressed as fractions of F_{max} and L_{ref}. Velocity of shortening was expressed as $L_{ref}{\cdot}s^{-1}$. Aggregate data were expressed as mean$\pm$SEM. ANOVA and regression analyses were accomplished using GraphPad Prism 5 (GraphPad Software, Inc., La Jolla, CA, USA). $p \leqslant 0.05$ was considered to be sufficient to reject the null hypothesis.

RESULTS

Muscle bundle properties and morphology

Human lungs were received from six donors with an average age of 25.8$\pm$2.8 yrs. After measurements of mechanical properties, muscle strips were fixed and stained with Masson's Trichrome for histological morphometry (n=4). From the histological sections, the cross-sectional area of the muscle was measured and compared to the entire tissue preparation (fig. 1a). The percentage of smooth muscle cross-sectional area to the total cross-sectional area of the tissue preparation averaged 36.5$\pm$0.04%. The maximal stress generated by the muscle averaged 82.1$\pm$17.3 $mN{\cdot}mm^{-2}$.

Ultrastructure

Muscle strips were also fixed for EM. A transverse electron micrograph of a muscle cell is shown in figure 1b. The cells are similarly ''packed'' within bundles like ASM from other species (fig. 1b), and share similar intracellular features. Like other mammalian ASM cells, human cells lack the well-organised arrays of contractile filaments seen in striated muscle (fig. 1b and c). Myosin thick filaments are present throughout the cell and are vastly outnumbered by actin filaments (fig. 1b and c). Areas of electron dense material, known as dense bodies and plaques, are also seen. Mitochondria, sarcoplasmic reticula, caveolae and microtubules are also present and are indistinguishable from their counterparts in animal cells.

Force–length properties and length adaptation

The relationship between muscle length and force-generating capacity was examined by recording force at five different lengths (fig. 2). Between shorter and longer lengths the muscle was returned to L_{ref} and re-equilibrated (fig. 2a). Immediately following a length change from L_{ref}, the active force declined and gradually recovered to a greater force over time (fig. 2b). On average, the active force did not fully recover to F_{max} at any of the lengths during the 20 min. Part of the incomplete recovery was due to a general force deterioration over the time course of the experiment. Correction for force deterioration was accomplished by assuming a linear decline and fitting a line through the first contraction at L_{ref} and the last (fifth) contraction after the length was returned to L_{ref} (force= -0.0006 $\times$ time + 1, where time is in minutes; suggesting an average decline of 10.8% from initial force after 3 h). This correction assumes that force at L_{ref} returns to F_{max} in the absence of deterioration, thus preventing an underestimation of force recovery (corrected values are presented in figs 2 and 3). To compare the extent of length adaptation, the initial force after a length change (first contraction) was compared to the final force measurement after the adaptation period (fifth contraction); this is displayed in figure 3. There was a significant length adaptation of active force over the 20-min period (fig. 3) ($p<0.0001$, ANOVA). Bonferroni post-tests demonstrated that active force at $0.50 \times L_{ref}$ and $1.50 \times L_{ref}$ were significantly greater after the period of

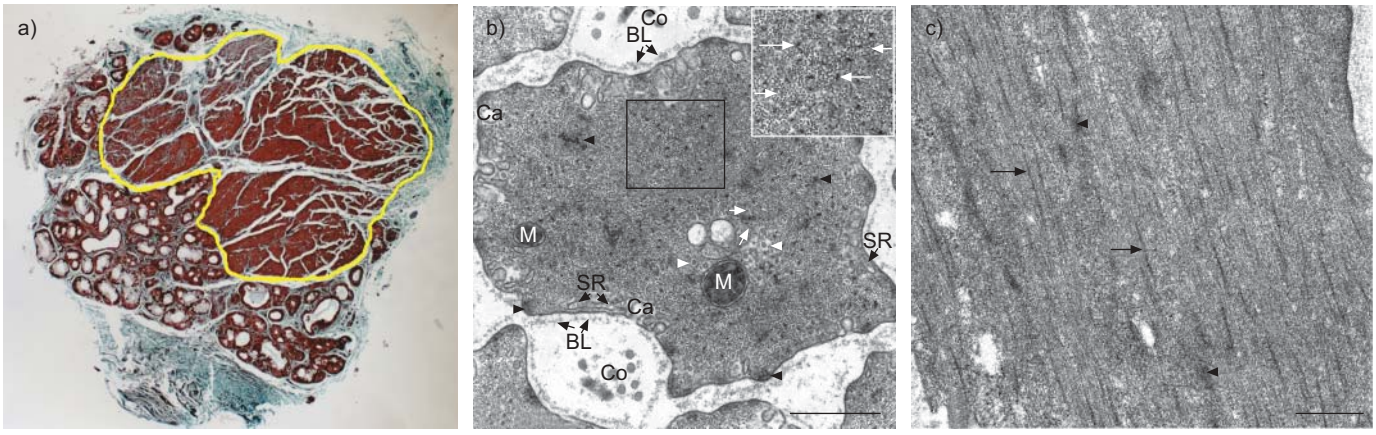

FIGURE 1. Morphology and ultrastructure of the airway smooth muscle (ASM). a) ASM strips were stained with Masson's Trichrome. The smooth muscle is red, connective tissue blue, and nuclei black. The yellow outline encircles the muscle bundles. The glandular, red staining cells were excluded. Morphometric analysis was used to determine the cross-sectional area of muscle in the dissected strip. This area was used to calculate the maximal stress generated by each smooth muscle preparation (stress is equal to force divided by cross-sectional area). Colour segmentation was used to exclude the blue connective tissue within muscle bundles. Image width 1.14 mm. b) Electron micrograph of an ASM cell sectioned transversally. Arrowheads indicate dense bodies (cytoplasmic) and dense plaques (membrane associated). White arrows indicate intermediate filaments; white arrowheads indicate microtubules. M: mitochondria; Ca: caveolae; SR: sarcoplasmic reticulum; BL: basal lamina; Co: collagen fibres. Inset panel shows a magnification of the square area shown. Small arrows indicate actin thin filaments and larger arrows indicate myosin thick filaments. Scale bar=0.5 μm. c) Electron micrograph of a longitudinal ASM cell section. Arrowheads point to dense bodies and arrows point to myosin filaments. Scale bar=0.5 μm.

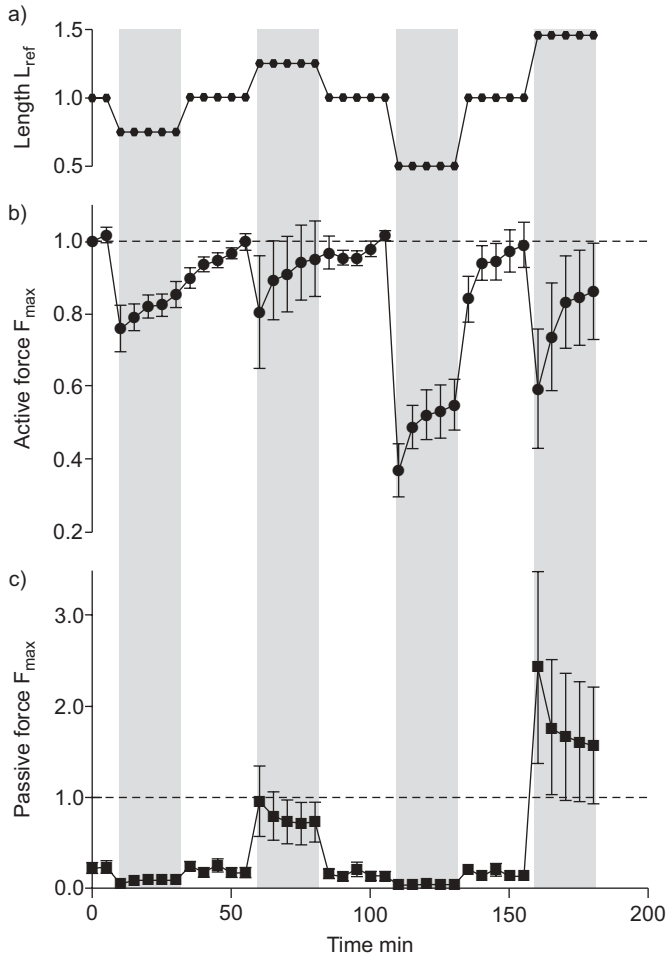

FIGURE 2. Isometric force at different lengths. a) The sequence and the time course of length changes are shown. Airway smooth muscle strips were either shortened or lengthened in the relaxed state to 0.50, 0.75, 1.25 or 1.50 L_{ref}. The muscle was stimulated to contract five times with electrical field stimulation at 5-min intervals after every length change (●). The force was corrected for force deterioration over time (see text for details). Between shortening and lengthening steps, the muscle was returned to, and readapted at, L_{ref}. The active force (b) and passive force (c) were recorded at every contraction. Error bars indicate SEM; n=6 from six different donors.

adaptation ($p<0.05$ and $p<0.001$, respectively). Passive force (figs 2c and 3) also demonstrated a significant length adaptation ($p=0.0053$, ANOVA). At lengths longer than L_{ref}, the passive force initially increased with the length change but decreased over the period of adaptation. Conversely, at shorter lengths, the passive force initially declined but gradually increased over the 20-min period. On average, the passive force did not reach pre-length change levels, despite significant adaptation (fig. 3).

Recovery from mechanical perturbation

The magnitude and time required for force recovery following a perturbation was examined by applying an oscillatory strain to the relaxed muscle. The 10 min length oscillation occurred at a frequency that mimics human breathing (0.2 Hz) and at a magnitude similar to deep inspiration

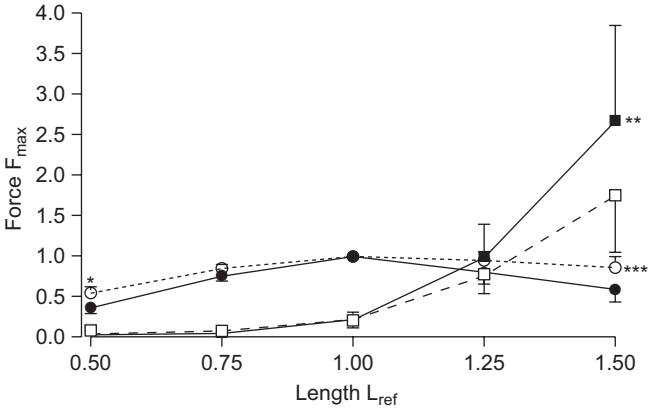

FIGURE 3. Active and passive force–length relationships before and after length adaptation. From L_{ref}, the airway smooth muscle strips were either shortened or lengthened to 0.50, 0.75, 1.25, and 1.50 L_{ref} (refer to fig. 2 for sequence and time course of length changes and stimulation). Active force (circles) and passive force (squares) both before (solid lines and closed symbols) and after (dashed lines and open symbols) length adaptation are shown. The force was corrected for deterioration over the time period of the experiment; see text for details. Active force before and after adaptation was length independent in the range 0.75–1.5 L_{ref} ($p<0.05$, ANOVA). Error bars indicate SEM; n=6 from six different donors. *: $p<0.05$; **: $p<0.01$; ***: $p<0.001$; adapted force compared to nonadapted force at a given length.

(30% L_{ref}). As seen in figure 4 (not corrected for force deterioration), immediately following oscillation the force decreased to 0.643 ± 0.03 F_{max} and recovered to 0.953 ± 0.03 F_{max} 30 min after oscillation.

Shortening velocity

Two sets of data were generated to examine the shortening velocity of human ASM. At both time points, the muscle was released to five different pre-determined loads (each representing a certain percentage of F_{max}). The difference between the two sets of data was the time of release (fig. 5). The late releases were performed during the tetanic plateau of active force, while the early releases were performed mid-way to the plateau (on average 3–4 s after the onset of stimulation). Both data sets were fitted with Hill's hyperbolic equation (fig. 6) [30]. Maximal shortening velocity, determined by Hill's equation, was 0.609 and 0.394 $L_{ref}{\cdot}s^{-1}$ for the early and late-phase, respectively. Force–velocity curves at the two time points were significantly different ($p<0.0001$, repeated measures ANOVA).

Maximal isotonic shortening

In four muscle preparations the extent of unloaded shortening was determined (fig. 7). Each ASM strip was allowed to isotonically shorten against a predetermined load (10% and 20% F_{max}). The maximal unloaded shortening was extrapolated from a linear regression of the points ($R^2=0.749$, $p=0.0055$). This regression assumes that the ascending limb of the force–length curve for a nonadapted muscle is linear [33]. The 95% confidence intervals ranged from 60.3 to 84.1% of shortening at zero load with an average of 72.2% (total length of the muscle).

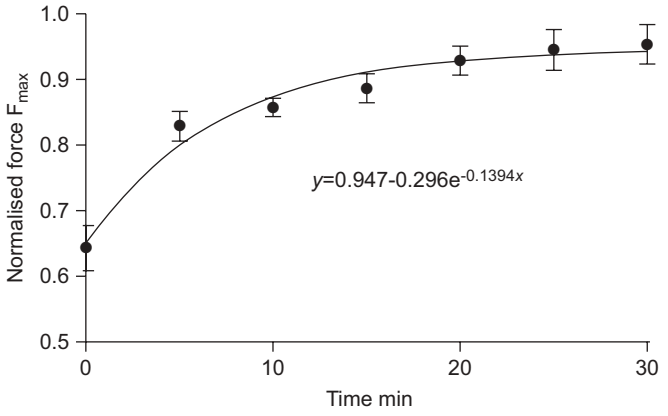

FIGURE 4. Isometric force recovery following a length oscillation. Recovery of isometric force following a 10 min, 0.2 Hz, 30% L_{ref} length oscillation. Airway smooth muscle strips were adapted to L_{ref} prior to the oscillation. The force produced by seven electrical field stimulation-induced contractions were recorded at 5-min intervals following the oscillation. Error bars indicate SEM; n=6; R^2=0.7254.

DISCUSSION

Despite the prominent role of ASM in airway diseases, the basic mechanical properties of human ASM have not been adequately determined. This study is the most comprehensive description of the mechanical properties of human ASM to date and is unique in that the experiments were performed within the paradigm of ASM mechanical plasticity using a high-quality tissue source. Our results demonstrate that human ASM possesses similar mechanical properties and morphological features as those found in other mammals such as dogs, pigs and sheep. This provides justification for using ASM tissues from non-human species to elucidate contractile mechanisms. Also, mechanical responses to experimental interventions in non-human mammalian ASM can now be justifiably interpreted in terms of human airway physiology. This study also provides a database of mechanical parameters for intact nonasthmatic human ASM, an invaluable reference against which asthmatic ASM can be compared.

Qualitatively, human ASM is indistinguishable from that of other species, as concluded from comparisons with ultrastructural images [25, 33–35]. The present study demonstrates the

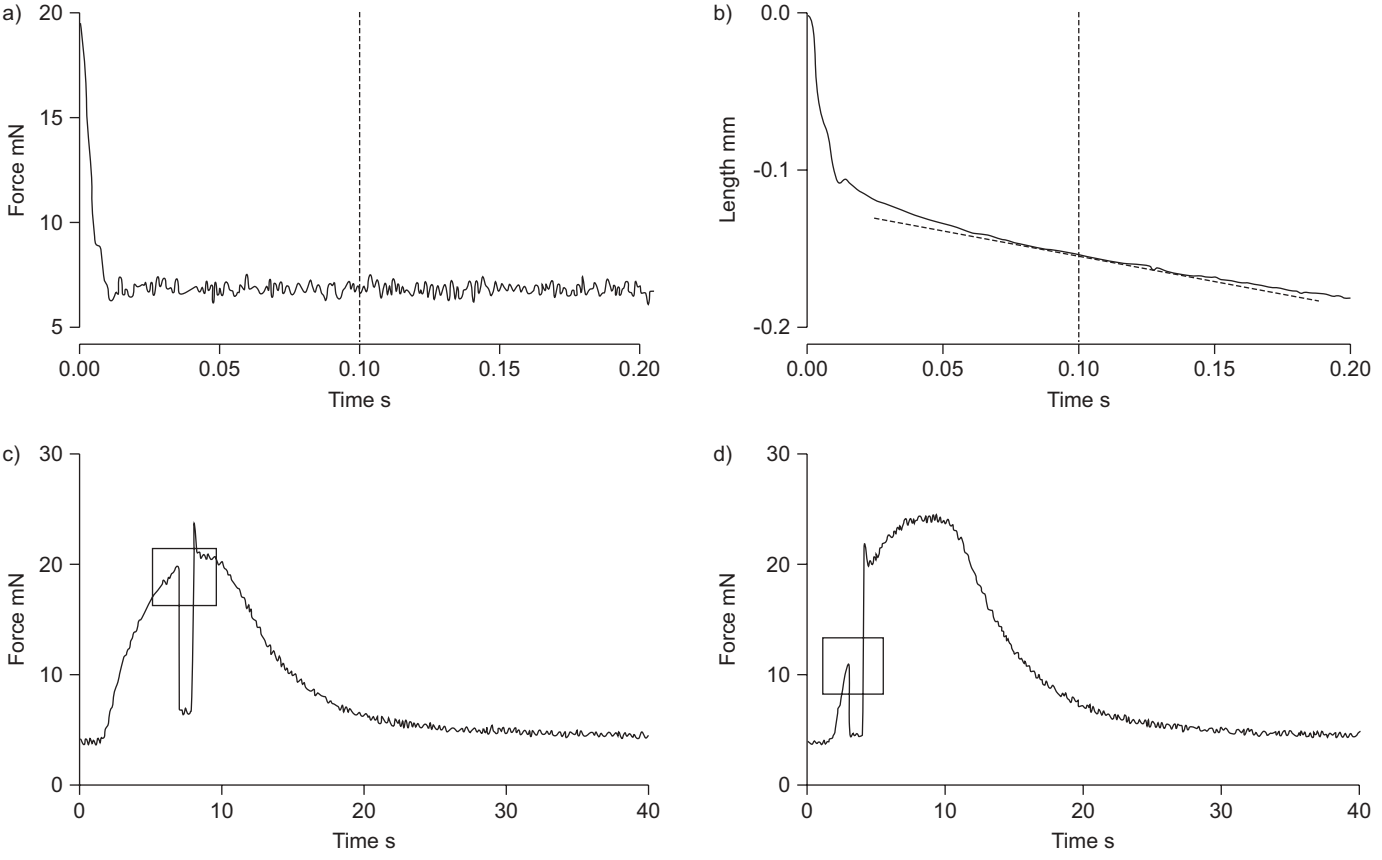

FIGURE 5. Determining shortening velocity during an isotonic contraction. Shortening velocity was determined at two time points during electrical field stimulation (c and d). A late load release was performed during the force plateau (c), while an early load release was performed midway to the force plateau (d). Representative traces of force and length records of an isotonic release are shown (a and b). The load against which the muscle contracted was reduced to a specific load in a time space of 10 ms (6 mN in the case shown here). The velocity was determined by calculating the slope of the tangent line during steady-state shortening at 100 ms. For each release, five different loads were used.

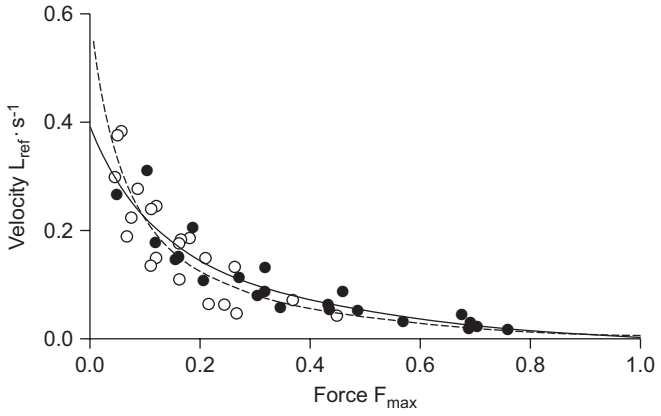

FIGURE 6. Isotonic shortening velocity measured against different loads at two time points. Isotonic shortening velocity was measured at five different loads both at the early and the late phase of contraction (refer to fig. 5 for an example of shortening velocity measurement). The loads were determined as a percentage of F_{max}. Late release (●) and early release (○) data were fitted with Hill's hyperbolic equation. n=5 from five different donors. Late-phase: R^2=0.8665; early-phase: R^2=0.8417. The two groups were significantly different, repeated measures ANOVA: p<0.0001.

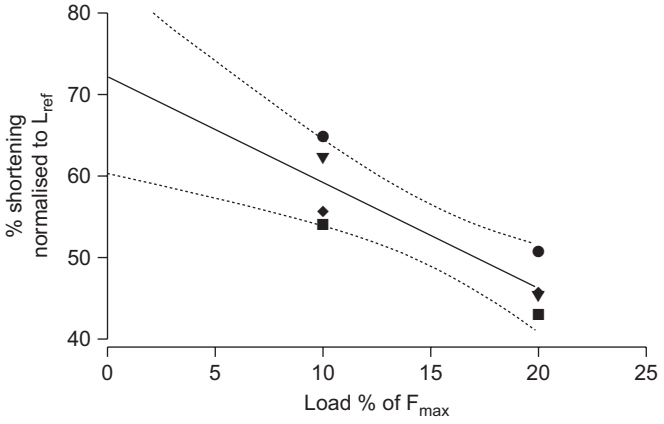

FIGURE 7. Maximal shortening. Airway smooth muscle strips were stimulated to contract with electrical field stimulation and the total amount of isotonic shortening against low loads was measured. Using the amount of shortening recorded at loads representing 10% and 20% of F_{max}, maximal shortening was extrapolated. Each symbol represents a muscle from a unique donor. n=4 from four different donors. R^2=0.7488, p=0.0055. - - - - -: 95% confidence intervals.

feasibility of quantitative comparisons of ultrastructural features (*e.g.* filament densities) and the relative abundance of mitochondria, caveolae, sarcoplasmic reticula, and other organelles of interest. Comparisons of these features will provide invaluable insights into the phenotypic changes associated with asthmatic ASM.

The results of previous studies suggested that human ASM possesses reduced stress generating capacity, reduced shortening capacity and greater passive stiffness compared with other species [5, 6]. Human ASM was found to generate a maximal stress of 50 ± 20 mN·mm^{-2} compared with 140, 72 and 80 mN·mm^{-2} in rabbit, dog and swine ASM, respectively [6]. The present results show that human ASM (82 ± 17.3 mN·mm^{-2}) generates stress that is comparable to dog and swine ASM. Another major finding of the present study is the ability of human ASM to undergo extensive shortening (72%) (fig. 7). This degree of shortening is similar to the reported values in other animal species, which range from 61 to 71%, and is much greater than the previously reported human ASM value of 25 ± 9.0% [6]. This discrepancy could be related to the reduced stress generated by the tissues in earlier studies which were dissected from bronchi obtained from surgical resections. In addition, the starting length of the muscle was set at L_{max}, an arbitrary length that is greatly influenced by the state of adaptation of the muscle [23].

Another difference in the present study, which could influence the degree of maximal shortening, was the percentage of muscle to total tissue area (36.49 ± 0.04%), which is much greater than the 8.7% reported in preparations from earlier human studies [5]. These data suggest that the previously studied human ASM was surrounded by a greater proportion of connective tissue, resulting in higher passive stiffness when compared with other species. Increased connective tissue could also prevent shortening by acting as a radial constraint and/or compressive load in parallel to the muscle cells [36]. This hypothesis is supported by the observation that treating human ASM preparations with collagenase led to a 50% increase in maximal isotonic shortening [11, 12]. Our carefully dissected tracheal preparations had similar ASM content to other non-human preparations that ranged from 25% to 35% smooth muscle area [6]. While the decreased connective tissue surrounding the muscle may have increased shortening in our study, it is unclear if passive tension was affected. In the previous study conducted at L_{max}, the passive tension in the muscle preparation was 60 ± 8.8% of maximal force [5]. In the present study average passive tension at L_{ref} was 22.4 ± 0.1% F_{max}.

Shortening velocity in smooth muscle peaks early in contraction, before force reaches a plateau; the velocity then decreases to a lower level after force plateaus and this velocity is maintained during the sustained phase of contraction. This decrease in velocity has been attributed to the development of latch-bridges caused by dephosphorylation of the myosin regulatory light chain in arterial muscle [37]. In non-human ASM, it has been proposed that the decreased velocity is likely due to thick filament lengthening during force development [28] and myosin phosphorylation was not found to correlate to velocity [38]. The present finding that velocity declines (fig. 6) during the time course of an isometric contraction suggests that myosin filaments in human ASM undergo similar rearrangements.

This is the first study to investigate whether length adaptation occurs in human ASM. Smooth muscle, like striated muscle, operates over a length range. In striated muscle, the force–length relationship is characterised by a well-defined optimal length where developed force is at its maximum. Outside the narrow plateau of maximal force, the force developed by the muscle decreases at shorter and longer lengths. This relationship depends on the overlap of the actin and myosin filaments within the muscle. Likewise, smooth muscle displays a force–length relationship that approximately

resembles a concave-down parabolic curve. However, ASM producing ''suboptimal'' force at a shorter or longer length can adapt to the new length, increasing its force within minutes [27]. This requires rearrangement of contractile and cytoskeletal proteins, and effectively broadens the force–length relationship of the smooth muscle [35, 39]. Thus, length adaptation allows smooth muscle to operate over the large length ranges seen *in vivo*, particularly in the smooth muscle tissues that line hollow organs that undergo large volume changes. Compared to previous studies in canine ASM [27] our data suggests that human ASM is less adaptable; that is, the length range of the force plateau in human ASM is smaller than that of canine ASM. Nevertheless, maximal force in human ASM is length-independent over the range of 0.75–1.5 L_{ref} ($p<0.05$, ANOVA), a clear sign that human ASM is capable of length adaptation (fig. 3).

The ability of the muscle to undergo length adaptation suggests that human ASM is capable of the mechanical plasticity demonstrated in other mammalian species. This ability to rearrange intracellular elements to generate force is further supported by the muscle's response to length oscillation (fig. 4). Our laboratory has previously shown in swine tissue that an oscillatory strain causes a decrease in force immediately after oscillation, followed by an exponential force recovery that coincides with myosin filament reformation [32]. However, the magnitude of recovery is somewhat blunted in human ASM, since the force did not fully recover to F_{max}, as it does in swine. Likewise, the rate of recovery is slower, with a rate constant of 0.139 s^{-1} *versus* 0.234 s^{-1} in swine ASM [32]. Human ASM is also more easily perturbed, since the force produced by human ASM immediately after oscillation was 64% F_{max} compared with ~79% F_{max} in swine [32]. This implies that human ASM has a more labile intracellular structure that reorganises more slowly than ASM from other species. *In vivo*, this may be beneficial for maintenance of airway patency. Coupled with its reduced ability to undergo length adaptation, the force loss associated with oscillation could enhance and prolong the effectiveness of bronchoprotection provided by a deep inspiration [40, 41]. The increased sensitivity to mechanical perturbation could be related to differences in the muscle's contractile apparatus or due to differences in extracellular structures, perhaps exposing human ASM to greater internal forces than are seen by other species. Comparisons to ASM from asthmatic subjects are certainly needed.

Previous studies comparing asthmatic and nonasthmatic ASM mechanical properties have suggested increased contractility (force development or shortening) [12, 20, 22] or sensitivity to certain agonists in asthmatic ASM [12, 13, 17], while others have shown no differences [14–16, 18, 19, 21]. With respect to the current study, it is unclear whether these are true differences or due to the inexactness of using L_{max} to determine ''optimal force,'' since the velocity, extent of shortening, and sensitivity to an agonist [42] are all length dependent. Only two studies have normalised force to cross-sectional muscle area, concluding that asthmatics generate more stress than nonasthmatics [12, 22]. Based on the results of the present study we suggest that these investigators may have underestimated maximal stress and the extent of shortening, either because of the way L_{max} was determined or due to less than optimal tissue quality. However these factors may have equally affected asthmatics and nonasthmatics and thus would not alter their conclusions. Alternatively, it is possible that these factors could differentially affect asthmatic and nonasthmatic tissues and lead to (or conceal) differences between the two groups.

In conclusion, this study is the first comprehensive study of the mechanical properties of healthy human ASM sourced from an intact lung. We have demonstrated that human ASM has ultrastructural features and mechanical properties which are similar to other animal species and is capable of length adaptation. These results suggest that human ASM probably has the same intracellular organisation and undergoes the same processes of mechanical plasticity that have been identified in the ASM of other species.

SUPPORT STATEMENT

This work was supported by operating grants from Canadian Institutes of Health Research (CIHR; Ottawa, ON, Canada) (MOP-13271 and MOP-4725). L.Y.M. Chin is supported by an Alexander Graham Bell Graduate Scholarship from the Natural Sciences and Engineering Research Council of Canada (NSERC; Ottawa). Y. Bossé is supported by a fellowship from Fonds de la Recherche en Santé Québec (FRSQ; Montreal, QC, Canada) and a CIHR Strategic Training Initiative in Health Research-IMPACT fellowship. T.L. Hackett is supported by the Canadian Lung Association (Ottawa) and a CIHR Strategic Training Initiative in Health Research-IMPACT fellowship.

STATEMENT OF INTEREST

A statement of interest for P.D. Paré can be found at www.erj.ersjournals.com/misc/statements.dtl

REFERENCES

1 Seow CY, Fredberg JJ. Historical perspective on airway smooth muscle: the saga of a frustrated cell. *J Appl Physiol* 2001; 91: 938–952.
2 Mead J. Point: airway smooth muscle is useful. *J Appl Physiol* 2007; 102: 1708–1709.
3 Fredberg JJ. Counterpoint: airway smooth muscle is not useful. *J Appl Physiol* 2007; 102: 1709–1710.
4 An SS, Bai TR, Bates JH, *et al.* Airway smooth muscle dynamics: a common pathway of airway obstruction in asthma. *Eur Respir J* 2007; 29: 834–860.
5 Ishida K, Paré PD, Hards J, *et al.* Mechanical properties of human bronchial smooth muscle *in vitro*. *J Appl Physiol* 1992; 73: 1481–1485.
6 Opazo Saez AM, Schellenberg RR, Ludwig MS, *et al.* Tissue elastance influences airway smooth muscle shortening: comparison of mechanical properties among different species. *Can J Physiol Pharmacol* 2002; 80: 865–871.
7 De Jongste J, Mons H, Van Strik R, *et al.* Human small airway smooth muscle responses *in vitro*; actions and interactions of methacholine, histamine and leukotriene C4. *Eur J Pharmacol* 1986; 125: 29–35.
8 De Jongste JC, Mons H, Block R, *et al.* Increased *in vitro* histamine responses in human small airways smooth muscle from patients with chronic obstructive pulmonary disease. *Am Rev Respir Dis* 1987; 135: 549–553.
9 de Jongste JC, van Strik R, Bonta IL, *et al.* Measurement of human small airway smooth muscle function *in vitro* with the bronchiolar strip preparation. *J Pharmacol Methods* 1985; 14: 111–118.
10 Jongejan RC, de Jongste JC, van Strik R, *et al.* Measurement of human small airway smooth muscle function *in vitro*. Comparison

of bronchiolar strips and segments. *J Pharmacol Methods* 1988; 20: 135–142.
11 Bramley AM, Roberts CR, Schellenberg RR. Collagenase increases shortening of human bronchial smooth muscle *in vitro*. *Am J Respir Crit Care Med* 1995; 152: 1513–1517.
12 Bramley AM, Thomson RJ, Roberts CR, *et al.* Hypothesis: excessive bronchoconstriction in asthma is due to decreased airway elastance. *Eur Respir J* 1994; 7: 337–341.
13 Schellenberg RR, Foster A. *In vitro* responses of human asthmatic airway and pulmonary vascular smooth muscle. *Int Arch Allergy Appl Immunol* 1984; 75: 237–241.
14 Roberts JA, Raeburn D, Rodger IW, *et al.* Comparison of *in vivo* airway responsiveness and *in vitro* smooth muscle sensitivity to methacholine in man. *Thorax* 1984; 39: 837–843.
15 Cerrina J, Le Roy Ladurie M, Labat C, *et al.* Comparison of human bronchial muscle responses to histamine *in vivo* with histamine and isoproterenol agonists *in vitro*. *Am Rev Respir Dis* 1986; 134: 57–61.
16 Goldie RG, Spina D, Henry PJ, *et al. In vitro* responsiveness of human asthmatic bronchus to carbachol, histamine, beta-adrenoceptor agonists and theophylline. *Br J Clin Pharmacol* 1986; 22: 669–676.
17 de Jongste JC, Mons H, Bonta IL, *et al. In vitro* responses of airways from an asthmatic patient. *Eur J Respir Dis* 1987; 71: 23–29.
18 Whicker SD, Armour CL, Black JL. Responsiveness of bronchial smooth muscle from asthmatic patients to relaxant and contractile agonists. *Pulm Pharmacol* 1988; 1: 25–31.
19 Cerrina J, Labat C, Haye-Legrande I, *et al.* Human isolated bronchial muscle preparations from asthmatic patients: effects of indomethacin and contractile agonists. *Prostaglandins* 1989; 37: 457–469.
20 Bai TR. Abnormalities in airway smooth muscle in fatal asthma. *Am Rev Respir Dis* 1990; 141: 552–557.
21 Bai TR. Abnormalities in airway smooth muscle in fatal asthma. A comparison between trachea and bronchus. *Am Rev Respir Dis* 1991; 143: 441–443.
22 Thomson RJ, Bramley AM, Schellenberg RR. Airway muscle stereology: implications for increased shortening in asthma. *Am J Respir Crit Care Med* 1996; 154: 749–757.
23 Bai TR, Bates JH, Brusasco V, *et al.* On the terminology for describing the length-force relationship and its changes in airway smooth muscle. *J Appl Physiol* 2004; 97: 2029–2034.
24 Hackett TL, Shaheen F, Johnson A, *et al.* Characterization of side population cells from human airway epithelium. *Stem Cells* 2008; 26: 2576–2585.
25 Ali F, Chin L, Paré PD, *et al.* Mechanism of partial adaptation in airway smooth muscle after a step change in length. *J Appl Physiol* 2007; 103: 569–577.
26 Bossé Y, Chin LY, Paré PD, *et al.* Adaptation of airway smooth muscle to basal tone: relevance to airway hyperresponsiveness. *Am J Respir Cell Mol Biol* 2009; 40: 13–18.
27 Pratusevich VR, Seow CY, Ford LE. Plasticity in canine airway smooth muscle. *J Gen Physiol* 1995; 105: 73–94.
28 Seow CY, Pratusevich VR, Ford LE. Series-to-parallel transition in the filament lattice of airway smooth muscle. *J Appl Physiol* 2000; 89: 869–876.
29 Seow CY, Stephens NL. Force-velocity curves for smooth muscle: analysis of internal factors reducing velocity. *Am J Physiol* 1986; 251: C362–368.
30 Hill AV. The heat of shortening and the dynamic constants of muscle. *Proc R Soc London B Biol Sci* 1938; 126: 136–195.
31 Syyong H, Cheung C, Solomon D, *et al.* Adaptive response of pulmonary arterial smooth muscle to length change. *J Appl Physiol* 2008; 104: 1014–1020.
32 Kuo KH, Wang L, Paré PD, *et al.* Myosin thick filament lability induced by mechanical strain in airway smooth muscle. *J Appl Physiol* 2001; 90: 1811–1816.
33 Herrera AM, McParland BE, Bienkowska A, *et al.* ''Sarcomeres'' of smooth muscle: functional characteristics and ultrastructural evidence. *J Cell Sci* 2005; 118: 2381–2392.
34 Herrera AM, Martinez EC, Seow CY. Electron microscopic study of actin polymerization in airway smooth muscle. *Am J Physiol Lung Cell Mol Physiol* 2004; 286: L1161–L1168.
35 Kuo KH, Herrera AM, Wang L, *et al.* Structure-function correlation in airway smooth muscle adapted to different lengths. *Am J Physiol Cell Physiol* 2003; 285: C384–C390.
36 Paré PD, McParland BE, Seow CY. Structural basis for exaggerated airway narrowing. *Can J Physiol Pharmacol* 2007; 85: 653–658.
37 Dillon PF, Aksoy MO, Driska SP, *et al.* Myosin phosphorylation and the cross-bridge cycle in arterial smooth muscle. *Science* 1981; 211: 495–497.
38 Mitchell RW, Seow CY, Burdyga T, *et al.* Relationship between myosin phosphorylation and contractile capability of canine airway smooth muscle. *J Appl Physiol* 2001; 90: 2460–2465.
39 Gunst SJ, Meiss RA, Wu MF, *et al.* Mechanisms for the mechanical plasticity of tracheal smooth muscle. *Am J Physiol* 1995; 268: C1267–C1276.
40 Skloot G, Permutt S, Togias A. Airway hyperresponsiveness in asthma: a problem of limited smooth muscle relaxation with inspiration. *J Clin Invest* 1995; 96: 2293–2403.
41 Moore BJ, Verburgt LM, King GG, *et al.* The effect of deep inspiration on methacholine dose-response curves in normal subjects. *Am J Respir Crit Care Med* 1997; 156: 1278–1281.
42 Bosse Y, Chin LY, Pare PD, *et al.* Chronic activation in shortened airway smooth muscle: a synergistic combination underlying airway hyperresponsiveness? *Am J Respir Cell Mol Biol* 2010; 42: 341–348.